Nuclear Inst. and Methods in Physics Research, A 894 (2018) 25–32

Contents lists available at ScienceDirect

Nuclear Inst. and Methods in Physics Research, A

journal homepage: www.elsevier.com/locate/nima

Drive beam stabilisation in the CLIC Test Facility 3

L. Malina [a,b,*], R. Corsini [a], T. Persson [a], P.K. Skowroński [a], E. Adli [b]

[a] CERN, Geneva 23, Switzerland
[b] University of Oslo, 0316 Oslo, Norway

ARTICLE INFO

Keywords:
CLIC
CLIC test facility
Beam stabilisation
Beam-based feedback
Feedback

ABSTRACT

The proposed Compact Linear Collider (CLIC) uses a high intensity, low energy drive beam to produce the RF power needed to accelerate a lower intensity main beam with 100 MV/m gradient. This scheme puts stringent requirements on drive beam stability in terms of phase, energy and current. The consequent experimental work was carried out in CLIC Test Facility CTF3. In this paper, we present a novel analysis technique in accelerator physics to find beam drifts and their sources in the vast amount of the continuously gathered signals. The instability sources are identified and adequately mitigated either by hardware improvements or by implementation and commissioning of various feedbacks, mostly beam-based. The resulting drive beam stability is of 0.2°@ 3 GHz in phase, 0.08% in relative beam energy and about 0.2% beam current. Finally, we propose a stabilisation concept for CLIC to guarantee the main beam stability.

1. Introduction

The compact linear collider (CLIC) [1] is a proposed particle accelerator, which will possibly take over from Large Hadron Collider (LHC) at the high energy physics frontier after its planned shut down around 2035. CLIC is a linear e^+e^- collider with a centre of mass energy up to 3 TeV. To reach this energy, it will employ a two-beam acceleration scheme [1]. CLIC Test Facility CTF3 [2] is a test facility, which aims to demonstrate the feasibility of CLIC technology by generation of the high current drive beam used for two-beam acceleration and to develop a variety of different CLIC specific equipment.

The two-beam acceleration concept imposes strict requirements on the drive beam stability, in terms of current, energy and phase. The drive beam current stability impacts the stability of the main beam and it is critical for the integrated luminosity. The beam stability goals are defined as the values yielding 1% luminosity loss. The CLIC drive beam stability goals (phase translated to CTF3 machine independent of RF-frequency) are following [3]:

- beam phase of 0.2° at 3 GHz before phase-feed-forward (PFF)
- relative beam energy stability of 1×10^{-3}
- drive beam current stability of 7.5×10^{-4}.

The layout of CTF3 is shown in Fig. 1. A thermionic gun produces 1.3 μs long pulses of a 5 A continuous electron beam. The injector consists of 3 Sub-Harmonic-Bunching cavities (SHB) operating at 1.5 GHz, 3 GHz pre-buncher, buncher and 2 accelerating structures. The bunch frequency can either be 1.5 GHz or 3 GHz if the SHBs are disabled. It is one of the parameters defining the mode of operation: full factor 8 beam recombination is possible only with a 1.5 GHz beam, while 3 GHz allows only for factor 4. The bunched beam then passes through a magnetic chicane and about 4.3 A is accelerated in the 70 m long linac to the energy of 135 MeV. The acceleration of the beam is done with 3 GHz RF. The power is generated by klystrons delivering 5.5 μs and 40 MW pulses. Pulse compressors are employed to provide a flat-top of 80 MW and 1.4 μs. There are 16 accelerating structures operated in fully loaded mode [4]. This gives a high RF to beam efficiency, however, it introduces a strong correlation between the beam current and beam energy. In the delay loop, the beam pulse is converted to four 140 ns pulses of double intensity and bunch spacing by interleaving bunches using transverse RF deflectors. The four pulses are combined into a single one in the combiner ring. The beam is transported towards the experimental area CLEX [2], where it can be sent in the Test Beam Line (TBL), which investigates the effect of deceleration of the drive beam, or in the Two Beam Module (TBM), which experimentally verifies the concept of the two-beam acceleration.

In order to achieve the stringent stability levels needed for present and future machines, complex feed-back systems are usually required [5–9]. In Section 2 we describe the tools and algorithms that allow identification and study of the sources of drifts and jitters during machine operation. Section 3 describes a novel statistical analysis that

* Corresponding author at: CERN, Geneva 23, Switzerland.
E-mail address: lukas.malina@cern.ch (L. Malina).

https://doi.org/10.1016/j.nima.2018.03.057
Received 23 January 2018; Received in revised form 14 March 2018; Accepted 16 March 2018
Available online 27 March 2018

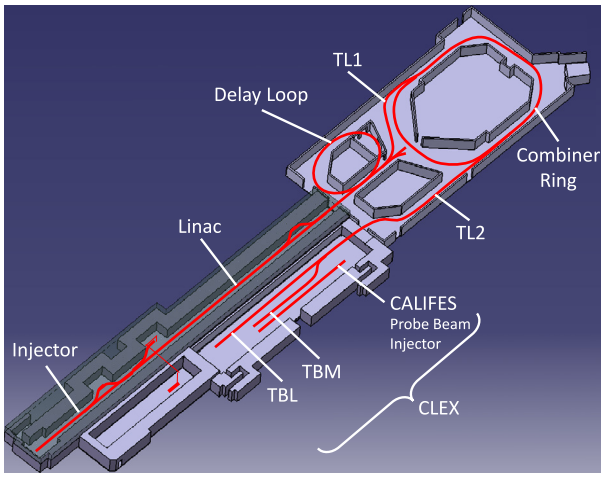

Fig. 1. Layout of CTF3.

allows identification of all relevant drifts within the very large amount of data recorded from hundreds of devices. The analysis leads typically to one of the following outcomes: identification of a particular hardware failure, which needs to be fixed, or to improved understanding of principles governing how to better stabilise the beam using a feedback system. The feedback systems developed for the CTF3 machine are described in detail in Section 4. In Section 5 the resulting beam stability is shown and discussed.

2. Monitoring and operational tools

In this section, we describe the monitoring and operational tools used in the CTF3 machine to identify failures and machine settings changes. In a single beam-pass machine, a change of the initial beam parameters affects all downstream beam parameters. It is therefore crucial to have precise control of the source and injector parameters. As an example, in CTF3 the phase and amplitude of the RF power in structures of the injector are one of the most critical parameters. Any change of these two parameters alters capture efficiency and therefore bunch charge. This also translates into a phase error after the magnetic chicane. Phase and charge differences modify the final bunch energy and length. This leads to different orbit and beam losses. Finally, the RF power produced by power extraction structures [10] has different amplitudes and phases.

In general, any observed drift at the end of a beam line can be caused by any of a vast amount of upstream signals, and the specific source is normally difficult to determine. In order to follow the evolution of all the signals and to provide input for the stability analysis of such complex system, two dedicated monitoring applications have been developed for machine operation.

The first one is called ReferenceMonitor and it is fully described in [11]. It shows in real time most of the beam related signals acquired along the beam pulse (hereafter referred to as "traces") together with earlier captured reference signals. Additionally, it displays the time evolution of their values averaged over the beam pulse and the χ^2 with respect to the reference. More importantly, it saves all beam related signals for further analysis. Since saving all traces for every pulse is not possible due to large amount of data, it saves the mean and χ^2 values instead. Full traces are saved periodically every 10 to 20 min.

For beam stabilisation in a given working point (the set of beam conditions along the machine), a change of the working point must be first effectively identified. An online watchdog application has been developed to quantify and determine the sources of the drifts. It compares the machine settings and the beam measurements to reference values. It shows the largest deviations measured by χ^2 in continuously updating fixed-displays. The signals are grouped by their type and are sorted according to their location along the machine layout. For clarity, only the locations with a beam presence are shown. This allows for quick identification of the origin of a drift, or at least its approximate location, by pointing out the most upstream signal that is diverging. The signal and its time evolution can be then verified in detail using the ReferenceMonitor. This makes these applications crucial for stabilisation of the machine since operators can more quickly identify a problem, determine the origin and react appropriately.

3. Drift and correlation analysis

Due to the large amount of recorded signals, drifts and jitters are analysed offline to identify the source and quantify the effect. This in turn defines the requirements for an appropriate feedback, specifically: required accuracy of signal acquisition, averaging time and gain. A dedicated algorithm has been developed to study drifts and jitters using the sample correlations between signals in a sliding time window of chosen length (depending on which time scale correlated signals are to be found). Let r be the correlation coefficient of pairs of normally distributed observables x and y:

$$r = \frac{\sum_{i=1}^{n}\left(x_i-\bar{x}\right)\left(y_i-\bar{y}\right)}{\sqrt{\sum_{i=1}^{n}\left(x_i-\bar{x}\right)^2}\sqrt{\sum_{i=1}^{n}\left(y_i-\bar{y}\right)^2}}, \tag{1}$$

where n is a sample size, $\bar{x} = \sum_{i=1}^{n} x_i$ and $\bar{y} = \sum_{i=1}^{n} y_i$. The sample correlation coefficient r lies in the interval $(-1;1)$. In order to easily work with significance levels, Fisher z-transform [12] is performed to obtain corresponding normally distributed quantity z and its uncertainty se:

$$z = \tanh^{-1} r = \frac{1}{2}\ln\left(\frac{1+r}{1-r}\right)$$

$$se = \sqrt{\frac{1}{n-3}}$$

The confidence interval $\left(r_-; r_+\right)$ for r (asymmetric in general) is obtained by back-transforming $z \pm se$. Nevertheless, this procedure would be biased, where n is small or r is close to ± 1, because a finite sample of normal distribution follows the student t-distribution. The latter case is not important for drift detection since the resolution for high correlations is not needed. A correction for small sample size (given the requested confidence level) follows:

$$z \pm \sqrt{\frac{1}{n-3}} \cdot f\left(1-\alpha, n-2\right),$$

where f is inverse of cumulative student t-distribution function, given the confidence level α. We treat the correlation as non-significant if zero is within the back-transformed $\left(r_-; r_+\right)$ interval. It is practical to define a measure $R^2_{non\text{-}zero}$, which is similar to the coefficient of determination R^2:

$$R^2_{non\text{-}zero} = sgn\left(r_+\right) \cdot sgn\left(r_-\right) \cdot \min\left(r_+^2, r_-^2\right), \tag{2}$$

which is positive only if the correlation coefficient is statistically inconsistent with zero at the chosen confidence level. R^2 quantifies the fraction of a signal B variation that can be explained by another signal A change. If $R^2_{non\text{-}zero}$ is positive, it directly implies lower estimate on a fraction of signal B variation explainable by signal A. This represents a robust measure, which can be used to filter a large amount of signal pairs in long data samples. This is especially important for a large-scale machine, such as CLIC. Typically the beam passes through periods of drift (signals strongly correlated with time) and periods of relative stability (the signal variations are dominated by noise). It is convenient to study the correlations at various fixed time scales, typically a few minutes to several hours. A drifting signal together with calculated sample correlation coefficients (with time) and respective $R^2_{non\text{-}zero}$ is shown in Fig. 2. We introduce a "movie" of a visualised matrix (devices vs devices) of $R^2_{non-zero}$s over a sliding time interval. Sample frame of the matrix of lower limits on coefficients of determination is shown in Fig. 3.

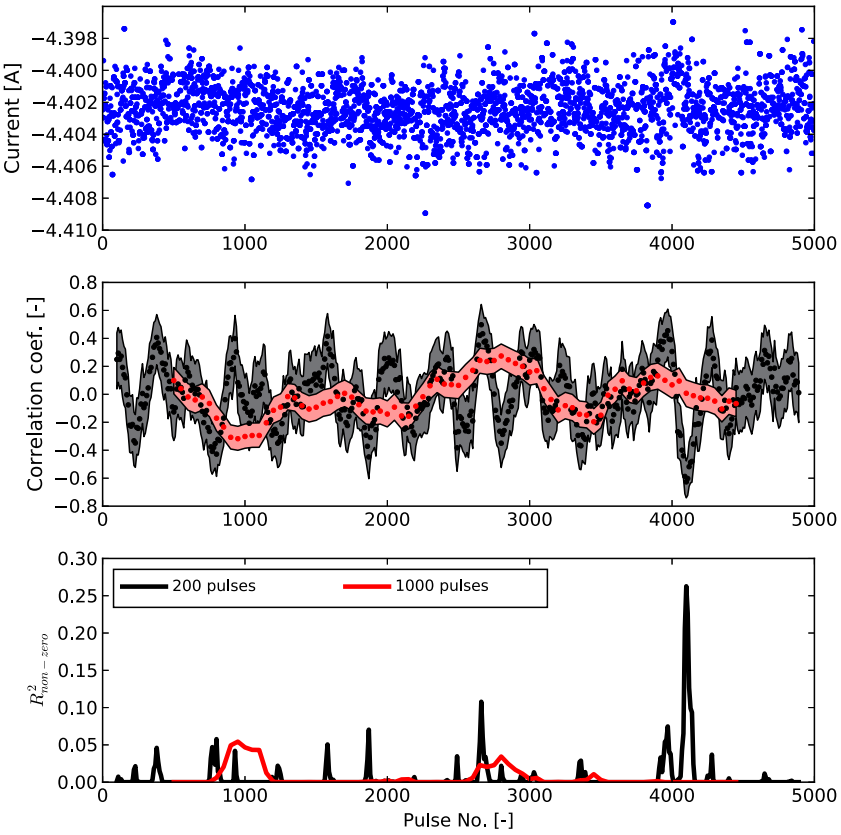

Fig. 2. In the top plot, a time evolution of a beam current signal is shown, its sample correlation coefficients with time over sliding time window (of two different lengths: 200 and 1000 pulses) is shown in the middle together with its confidence interval bands. In the bottom plot, the respective $R^2_{non\text{-}zero}$ is shown for given confidence level of two sets of correlation coefficients.

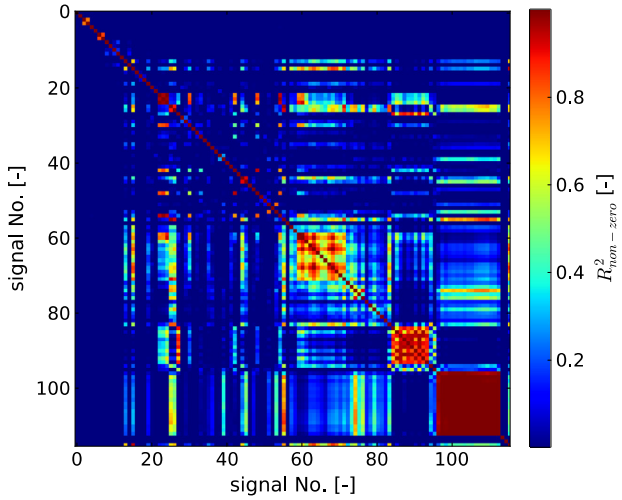

Fig. 3. Sample frame of the matrix of lower limits on coefficients of determination among devices along the beam line in a sliding time window.

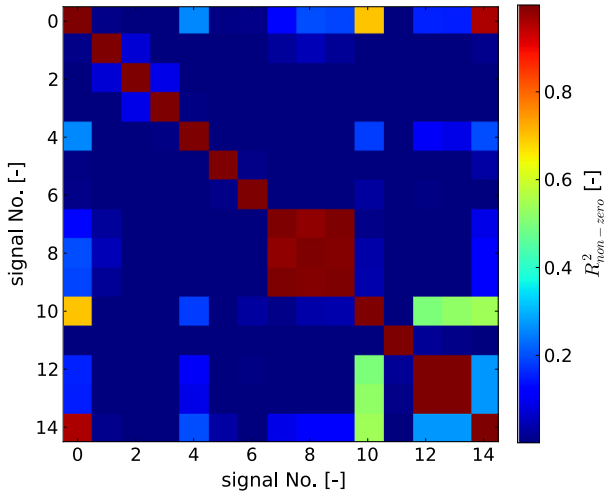

Fig. 4. Sample frame of the matrix of lower limits on coefficients of determination among a small subset of devices, directly corresponding to physical observables, in a sliding time window. A beam current (signal No. 0) drift, i.e. high correlation with time (signal No. 14), causes the downstream parameters to change. Due to full beam loading in the linac, the beam energy changes (signal No. 10), while the beam phase is almost intact (signals No. 4 and 8). The consequent beam energy drift changes the extraction efficiency from CR, i.e. the beam current in TL2 and TBM (signals No. 12 and 13) is correlated to beam energy.

A small subset of signals is shown in Fig. 4, demonstrating the changes of downstream observables caused by a beam current (signal No. 0) drift, i.e. high correlation with time (signal No. 14). Due to full beam loading in the linac, the beam energy changes (signal No. 10), while the beam phase is almost intact (signals No. 4 and 8). The consequent beam energy drift changes the extraction efficiency from CR, i.e. the beam current in TL2 and TBM (signals No. 12 and 13) is correlated to beam energy.

4. Stabilisation systems

Direct observation of the recorded signals lead to the implementation of the following RF feedbacks:

- RF phase loops
- ambient temperature feedback in the RF pulse compression system
- RF power flattening feedback.

The RF feedbacks detailed above improved beam stability by more than one order of magnitude and are summarised in Table 1. To further improve beam stability, an extensive signal correlation study pointed out a need for additional beam-based feedback systems:

- gun current stabilisation feedback
- injector feedback, which stabilises the beam phase
- loading feedbacks, which mainly stabilise the phase and remove the correlation between the beam current and energy
- energy flattening feedback, which flattens the beam energy along the pulse.

These feedback systems are described below, together with the treatment of potential cross talks among different systems.

All the CTF3 feedback systems are designed in a fail-safe manner. They do not act unless all control parameters are within tolerances defined at the time of commissioning and calibration of the system. In particular, they are active only when sufficient beam current is confirmed by the first beam position monitor (BPM) downstream from the location of the signal that is being stabilised. Injector and loading feedbacks also check whether the RF power delivered by the associated klystrons is close enough to the reference value. Experience showed that reaching the reference working point is impossible when the difference is bigger than 1 MW and an attempt to compensate it by adjusting RF phases or gun current would result in significant beam losses.

The beam pulse length varies significantly in operation of CTF3 drive beam, as it consists of different beam setups and experiments. The feedbacks also follow changes of the beam pulse length and automatically adapt the reference ranges. For that reason, the feedbacks are always calibrated with the longest possible beam pulse. When the start or end time of a beam pulse is changed, the feedbacks recompute all the required variables using only the overlapping part of the actual beam pulse and the reference measurement. Therefore, neither recalibration nor a new reference measurement is needed. Thanks to this feature the feedbacks can be used to automatically restore the beam conditions during restart. They proved to be very efficient and even in cases of longer shutdowns, when the RF phases and the current of the gun drifted to basically random values, they were able to bring back the beam to the reference conditions within hundreds of pulses.

4.1. RF-feedbacks

The RF pulse compression [13–15], which increases the RF peak power in CTF3 linac, is very temperature sensitive. Even though the cooling water temperature of the RF compressors was stabilised to 0.05 °C, residual variations coming from the klystrons, waveguides and originating from ambient temperature changes in the klystron gallery influenced the shape of the compressed pulse. For this reason, a temperature feedback was implemented to dynamically correct the setpoint of the water-cooling station for each compressing cavity [16].

In order to further stabilise RF phase and power, additional feedback systems are implemented. The amplitude of the compressed RF pulse is controlled by RF phase at the input of the compressing cavity. It is derived with a non-trivial iterative algorithm [17]. A part of this algorithm was programmed into a feedback loop in order to preserve the pulse amplitude [18] (RF pulse flattening). It stabilises not only the mean power, reducing the mean beam energy drifts, but also the amplitude along the pulse, stabilising the energy of the bunches along the train. The phase of the RF is stabilised using phase loops, which keep constant the RF phase measured after the pulse compressor [16]. They need to act fast enough to correct the phase errors introduced by the RF pulse flattening. Phase-locked loops are also implemented in the travelling wave tubes (TWTs) in the injector. However, the measurements used in the feedbacks are temperature sensitive as well. For example, day/night temperature variations are pronounced during summer, when air-conditioning capacity is insufficient to prevent the temperature raise.

This results in long-term variations of the phase working points, which need to be mitigated by beam-based feedbacks described below. Fig. 5 shows the CTF3 injector and linac layout including the beam-based feedback measurement locations and Table 2 summarises the control settings used to stabilise them.

4.2. Beam current and phase stabilisation

The beam current is stabilised using the BPM located at the end of injector because it offers much more accurate current measurement comparing to the devices installed upstream. At this location, the beam is fully relativistic, which allows use of an inductive wall current monitor. Such a device is much more reliable compared to the electrostatic devices installed within the injector, which suffer from a large droop and are heavily influenced by charging-up from the electrons scattered in the bunching cavities. The feed-back loop is closed on the gun pulser intensity knobs (fine and coarse), that regulate the grid voltage in the thermionic gun.

The beam phase is predominantly defined by the injector, where the electrons become ultra-relativistic. Further downstream, the beam phase is less influenced by accelerating RF, especially when the lattice is correctly tuned with the nominal $R_{56} = 0$ m. Two Beam Phase Reference (BPR) monitors are installed in the injector to measure bunch phase and length, see Fig. 5). The bunch length measurement is only relative because the signals have strong non-linear dependence on bunch charge and position. It is, therefore, important to monitor that these parameters are constant.

The injector feedback stabilises the longitudinal beam parameters as measured by the two BPRs. The main part of the feedback system is common for both 1.5 and 3 GHz bunch frequency modes. Different configurations were verified and the best performance is achieved when

- Phase of the klystron 3 is used to stabilise the bunch length signal of the downstream monitor (BPR0475).
- Simultaneous phase change of both klystrons 2 and 3 is used to stabilise phase signal of the upstream monitor (BPR0290). Such correction does not modify the bunch length at the downstream monitor because the relative phase between the cavities is left unchanged.

The second part of the feedback system acts only on the beam with 1.5 GHz bunching frequency and stabilises the phases of the travelling wave tubes (TWT) that power the SHBs. The system stabilises the RF power measured at the exit of SHB cavity in presence of the beam (i.e., beam loading measurement) and the BPR0290 bunch length measurement. As the proportionality ratios are subject to drifts it employs an automatic calibration procedure. In an optimised working point this feedback is linear in the first two phases and quadratic in the third. The feedback uses the acquired reference signals as a target for corrections using measured calibration factors. Both the reference signals and the calibration factors are beam-mode dependent.

As already mentioned, the bunch length measurement is sensitive to beam current (in principle proportional to beam current squared) and the deviation from the reference klystron phases with respect to the beam phase changes the amount of beam losses in the injector. This entangles the beam current and the beam phase. In order to avoid resonant cross-talks between the feedbacks, they work at different

Table 1
Measurements and steering knobs used in CTF3 RF feedback systems.

Feedback	Measurement	Knob
Phase-loops	Phase of compressed RF	Phase shifters
Ambient temperature	Pulse compressor temperatures	Temperature set point
RF flattening	Power amplitude of compressed RF	Waveform generator function

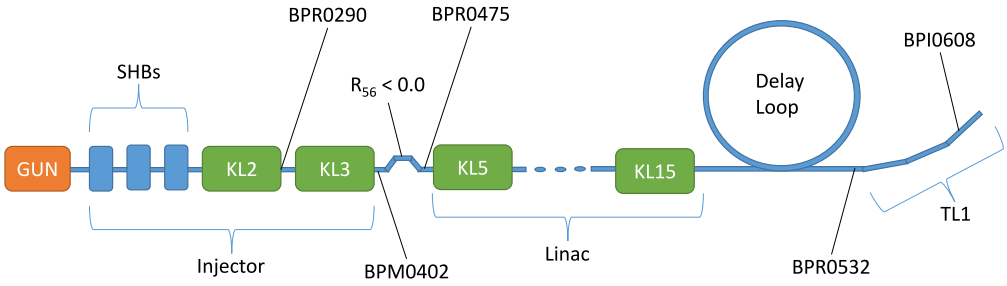

Fig. 5. Schematic view (not to scale) of the CTF3 injector and linac showing the locations of measurements, which are being stabilised, together with the knobs used to control them, listed in Table 2.

Table 2
Measurements and steering knobs used in CTF3 beam-based feedback systems. Their physical locations are shown in Fig. 5.

Feedback	Measurement	Knob
Gun current	BPM0402 — current	grid voltages of thermionic gun
Injector 3 GHz	BPR0290S BPR0475W	Klystron 2 phase Klystron 3 phase
Injector 1.5 GHz	TWT loadings BPR0290W	Phases of all three TWTs
Klystron Loading (5 to 15)	Accelerating structure loading	Klystron phase
Energy flattening	BPI0608H — dispersive BPI	Waveform klystron 15

time scales, i.e. integration times. Moreover, in case when the beam is restarted and the settings might have drifted away from references, the beam phase feedback is not acting for several pulses, waiting for the beam current being back at the reference value.

4.3. Beam energy stabilisation

After implementation of the RF power stabilisation system [18], the beam energy stability was improved to about 0.2% over several minutes, and over longer times up to about 2%. It was found that the remaining beam energy variations still caused beam intensity fluctuations through losses. The energy variations are mainly due to slow changes of sensitivity in RF phase and power measurements (e.g. temperature effects), upon which the phase loops and the RF power stabilisation feedback respectively rely. Further, any beam current variation affects the acceleration, for these reasons beam-based feedback systems are employed.

The CTF3 linac is operated close to fully loaded mode [4], therefore in most of the cavities the remaining power at the output port (referred to as loading) is measurable. A sample signal is shown in Fig. 6. This strongly depends on the phase between the electron bunches and the accelerating field. It is stabilised by loading feedbacks, which adjust the appropriate klystron phases. Loading feedbacks are implemented and commissioned for all the klystrons in the linac. The reference trace is an average of several traces acquired for a short period after the feedback is turned on. The construction of the penalty function is not trivial because simple difference or χ^2, even in the simplest case, is neither linear nor monotonous as the working point is close to full beam loading, where the loading shapes are complex (Fig. 6).

The feedback minimises a linear combination of χ^2 from the reference measurement (trace along the beam pulse) and the slope of the

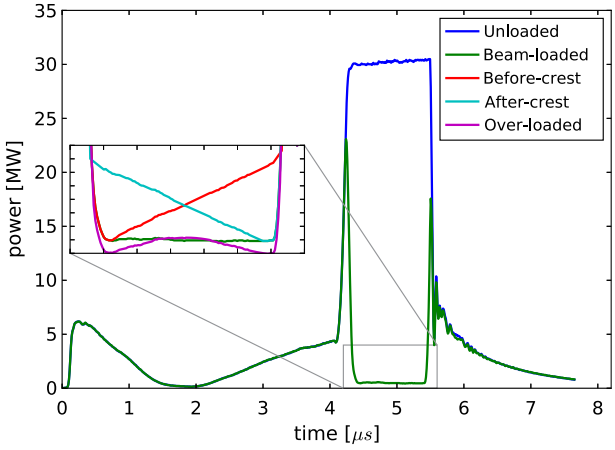

Fig. 6. The power measured at the exit of accelerating structure. In case of full beam loading the internal part of a pulse is close to zero. Sketches of different beam-loading patterns depending on relative phase and amplitudes between the RF and the beam-loading are shown in zoomed-in plot.

remaining power along the pulse:

$$p = \sum_{i=1}^{n} \left(x_{meas} - x_{ref}\right)^2 + C\left(\sum_{i=n-10}^{n} \left(x_{meas} - x_{ref}\right) - \sum_{i=1}^{10} \left(x_{meas} - x_{ref}\right)\right),$$

where C is a klystron-specific free parameter to make the penalty function a monotonous function of klystron phase deviation. Since the minimisation without gain setting is relatively slow, a higher gain mode

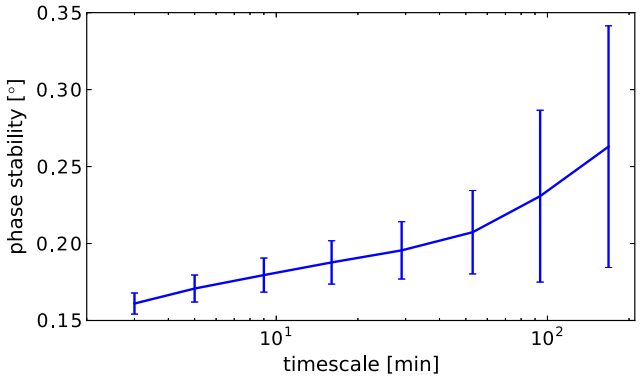

Fig. 7. Average beam phase stability measured at location BPR0532 as a function of the averaging time in the 3 GHz beam mode.

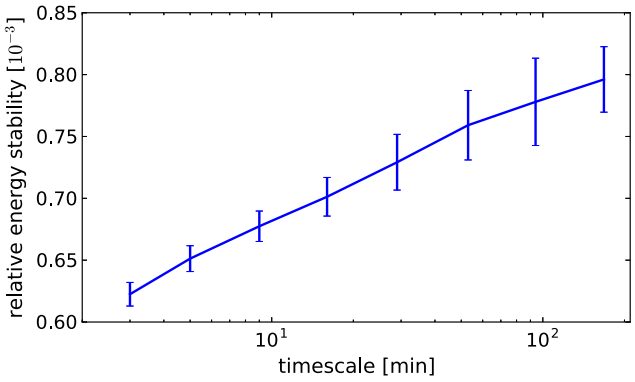

Fig. 8. Average relative beam energy stability measured at location BPI0608 as a function of the averaging time in the 3 GHz beam mode.

has been developed for more rapid drifts, i.e. when the beam condition gets further away from the reference, where it is not limited by noise. In such a case, the feedback measures the local penalty function derivative and performs a biased Newton iterative method minimisation. In other cases the feedbacks are limited by high noise and drifts of power measurements themselves, therefore they operate on scales of minutes rather than seconds.

In order to stabilise the beam energy along the pulse, which is disturbed by residual RF power variations added up through the acceleration, an energy flattening feedback was developed [9]. It is a variant of RF pulse flattening feedback that flattens the beam energy instead.

5. Beam stability

The CTF3 beam stability in various beam modes is quoted in this section in terms of drive beam phase, energy, current, and probe beam acceleration. Generally, we show the average stability (i.e. as opposed to best obtained stability) as a function of a time-scale (a period of time over which the stability is measured). The repetition time of CTF3 beam pulses is 1.2 s, thus stability over one hour means 3000 pulses.

The beam phase and energy variation is measured at BPR0532 and BPI0608 (see Fig. 5). The phase measurement is close to the upstream high-precision PFF phase monitors offering a resolution of 0.05° at 3 GHz [19]. At the location of BPI0608, there is a horizontal dispersion of 60 cm, therefore any change of energy is visible as a horizontal orbit change. It is verified with singular value decomposition of multiple BPMs that there is no significant dispersion upstream of the first bend that would modify the assumed value at BPI0608, and that incoming orbit and power supply jitters have negligible influence. Therefore, this signal represents well the beam energy.

The achieved beam phase stability is shown in Fig. 7 and is limited by the fluctuation of the phase measurements themselves. The fluctuations are likely caused by thermal effects in the distribution of a local oscillator signal for the mixers as a different levels of coupling between different measurements were observed. The relative mean energy variation is shown in Fig. 8. Both the phase stability and the relative mean energy variation of the uncombined beam are quoted in Table 3, together with relative energy variation along the pulse. The beam phase and energy stability is independent of the beam recombination factor. It remains unchanged further downstream in the machine due to absence of further acceleration and overall momentum compaction $R_{56} = 0$ m [20].

The current stability from the gun to the dump with a beam recombination factor 4 is shown in Fig. 9. Each blue line stands for a relative current stability (at a given BPM) over an hour of beam time with beam-based feedbacks running. Red lines stand for the same quantity without beam-based feedbacks. The green dashed line reflects the CLIC current stability goal. For the same period of time, we show

Table 3
Beam phase and energy stability over period of one hour.

Quantity	Stability over an hour
Phase [° @ 3 GHz]	0.2
Relative pulse-to-pulse energy [%]	0.07
Relative energy along the pulse [%]	0.08

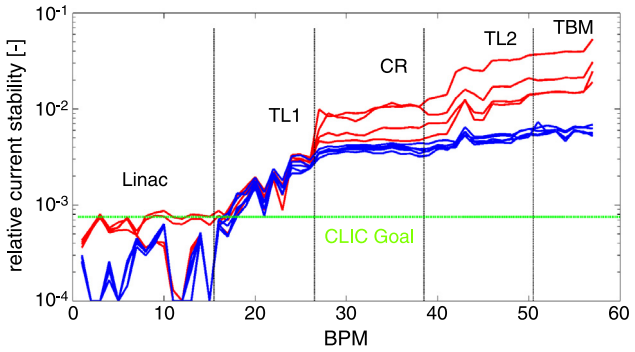

Fig. 9. Several sets of relative beam current stability measurement (combination factor 4) along the machine. Each line refers to stability over a period of one hour. In blue; beam-based feedbacks operating, in red: feedbacks turned off. The BPM noise is subtracted (in squares). The current variation in the linac is below the BPM resolution, causing the jagged structure of the lines. (For interpretation of the references to colour in this figure legend, the reader is referred to the web version of this article.)

in Fig. 10 the average relative beam current stability (in given a part of CTF3 with beam-based feedbacks operating) as a function of averaging time scale.

In the following we show the best average beam current stability in two typical operational modes:

- 3 GHz beam with multiplication factor 4 (not passing via Delay Loop) is shown in Fig. 11.
- 1.5 GHz beam with multiplication factor 8 is shown in Fig. 12.

In the first case, the beam has been well optimised and stability was limited by the resolution and stability of multiple measurements in the linac. For the 1.5 GHz beam, there were three main sources of difficulties:

- the time spent on optimisations and long stability studies of this beam was limited due to recurring failures of the TWTs
- the power supply of the septa magnet used for the injection to and extraction from the delay loop was jittering and could not be replaced with a better performing device

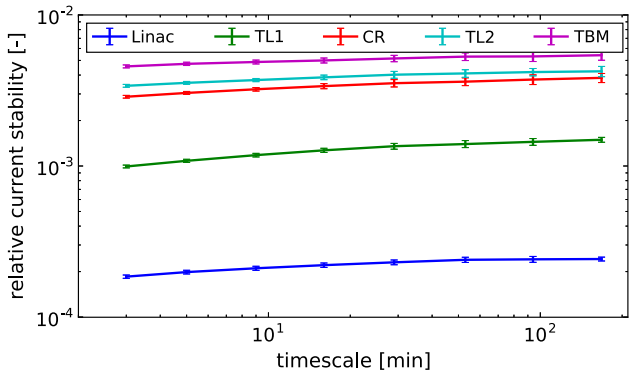

Fig. 10. Average beam current stability in different parts of the machine, as shown in Fig. 1, as a function of the averaging time for the very same data as in Fig. 9 (with beam-based feedbacks operating). For each machine part we use the average of several BPMs. The beam mode is 3 GHz beam with a recombination factor 4 in the combiner ring.

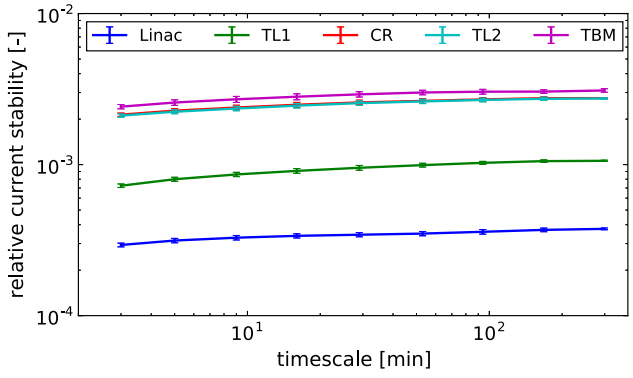

Fig. 11. Average beam current stability in different parts of the machine, as shown in Fig. 1, as a function of the averaging time. The beam mode is a recombination factor 4 in the combiner ring of 3 GHz beam.

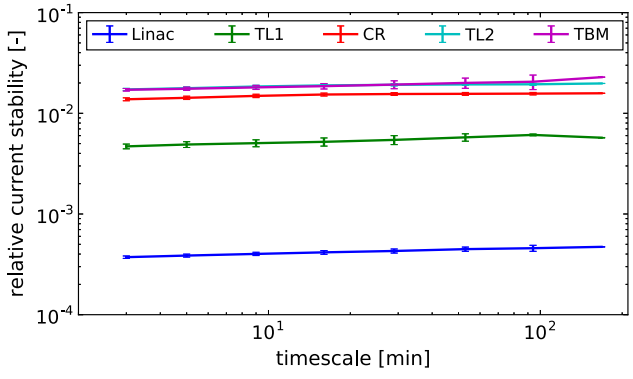

Fig. 12. Average beam current stability in different parts of the machine, as shown in Fig. 1, as a function of the averaging time. The beam mode is a recombination factor 8–2 in the delay loop and 4 in the combiner ring of 1.5 GHz beam.

- full transmission through the delay loop was not achieved since the strong isochronous optics of the delay loop limit momentum acceptance below the drive beam 0.6% r.m.s. energy spread. Unfortunately, due to the limited space in the pre-existing building, it was not possible to design weaker optics.

The main beam has been accelerated by the factor 8 combined drive-beam-generated RF power from the energy of 199 MeV to 242 MeV.

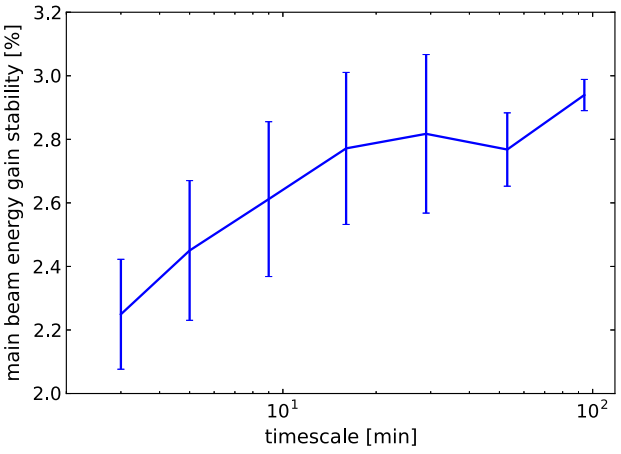

Fig. 13. The main beam energy gain stability while accelerated by RF coming from the factor 8 combined drive beam as a function of the averaging time.

Table 4
Achieved average drive beam stability compared to CLIC goals.

Quantity	Achieved	Goal
Phase [° @ 3 GHz]	0.2	0.2
Mean energy variation [%]	0.07	0.1
Energy variation along the pulse [%]	0.08	0.1
Current (linac) [%]	0.02–0.04	0.075
Current (after combination) [%]	0.2–1.8	0.075

The main beam energy was rather constant at the level of 1 MeV to be compared with typical spread of 0.6 MeV without the presence of drive-beam-generated RF power. The stability of the average energy gain of the main beam at different time scales is shown in Fig. 13. In the case of the factor 4 combined drive beam, the energy variation shows no increase (compared to case with no drive-beam-generated RF power). This shows that in such a case the drive-beam induced energy variation is much smaller than 0.6 MeV.

6. Conclusions and strategies for CLIC

In this paper, we focus on the beam stabilisation aspects of the CLIC drive beam complex. A novel analysis technique has been applied in detailed studies and allowed identification of the critical issues for beam stability. This algorithm, essential for the understanding of drifts and for latter implementation of feedback systems, is described in Section 3. Feedback systems to stabilise the drive beam have been designed and commissioned at CTF3. These feedback systems may also be useful in XFEL linacs, which operate in a similar mode to the CTF3 linac.

The achieved beam stability in CTF3 is summarised and compared to the CLIC drive beam stability goals in Table 4.

The CLIC goals have been reached in terms of beam phase (time of arrival), i.e. 0.2° at 3 GHz or 180 fs, before the final correction with the phase feed-forward (PFF) system. It must be noted that the PFF system showed a reduction of the incoming phase jitter to the final CLIC specifications (0.2° at 12 GHz, or 50 fs) thus validating the entire scheme [19]. Results below the CLIC requirements were also obtained for the mean beam pulse momentum stability and the momentum variations along the beam pulse. While the beam current in the linac was stabilised below the CLIC requirement as well, losses along the beam lines prevented this goal being reached for the combined beam, especially at its final destination in CLEX. There the average relative variation was 0.2%–1.8% depending on the beam mode, with the best stability being achieved for a combination factor 4 of the 3 GHz beam, the better known and used among the different operation modes. Given the much better beam size to aperture ratio of the CLIC beam lines with

respect to CTF3, the linac stability result constitute a reasonable proof-of-principle for the current stability in the overall drive beam complex of CLIC, where beam losses should be minimal.

The feedback systems developed at CTF3 are crucial for the CLIC drive beam stabilisation except for the RF pulse compression, which will not be used in CLIC. In the CLIC drive beam complex, the injector RF needs to be exceptionally stable. If possible, a solution like the one in CTF3, granting the same or better stability, should be implemented. This requires accurate beam instrumentation, especially for beam phase, current and acceleration cavity loading measurements. A general feedback framework needs to be embedded in the design of the machine and the control system, including the temperature measurements at all beam or RF related measurements. The monitoring application, together with the drift analysis framework need to be ready for the first beam commissioning in order to make the beam optimisation possible.

Acknowledgements

The authors would like to thank all CTF3 operators. We also would like to thank to Ewen Maclean for English language corrections.

References

[1] M. Aichler, P. Burrows, M. Draper, T. Garvey, P. Lebrun, K. Peach, N. Phinney, H. Schmickler, D. Schulte, N. Toge (Eds.), A Multi-TeV Linear Collider Based on CLIC Technology: CLIC Conceptual Design Report, Technical Report CERN-12-007, CERN, Geneva, Switzerland, 2012.

[2] G. Geshonke, A. Ghigo, CTF3 Design Report, Technical Report CERN-PS-2002-008-RF, CERN, Geneva, Switzerland, 2002.

[3] D. Schulte, et al., Status of the CLIC phase and amplitude stabilisation concept, in: LINAC'10, Tsukuba, Japan, 2010, pp. 103–105.

[4] R. Corsini, et al., First full beam loading operation with the CTF3 Linac, in: EPAC'04, Lucerne, Switzerland, 2004, pp. 39–41.

[5] R.L.A. Cottrell, C.A. Logg, M.J. Browne, A feedback system for steering and correcting the energy of the SLAC beam in the beam switchyard, Nucl. Instrum. Methods 164 (1979) 405–409.

[6] C. Schmidt, M.K. Bock, S. Pfeiffer, H. Schlarb, W. Koprek, W. Jalmuzna, Feedback strategies for bunch arrival time stabilization at FLASH towards 10 fs, in: FEL'11, Shanghai, China, 2011, pp. 531–534.

[7] S. Pfeiffer, C. Schmidt, M.K. Bock, H. Schlarb, W. Jalmuzna, G. Lichtenberg, H. Werner, Fast feedback strategies for longitudinal beam stabilization, in: IPAC'12, New Orleans, USA, 2012, pp. 26–28.

[8] S. Schulz, M.K. Czwalinna, M. Felber, P. Predki, S. Schefer, H. Schlarb, U. Wegner, Femtosecond-precision synchronization of the pump-probe optical laser for user experiments at FLASH, in: Proc SPIE 8778, Advances in X-ray Free-Electron Lasers II: Instrumentation, 87780R, Prague, Czech Republic, 2013.

[9] L. Malina, R. Corsini, D. Gamba, T. Persson, P.K. Skowronski, Recent improvements in drive beam stability in CTF3, in: IPAC'16, Busan, Korea, 2016, pp. 2677–2679.

[10] E. Adli, R. Ruber, V. Ziemann, R. Corsini, A. Dubrovskiy, I. Syratchev, X-band RF power production and deceleration in the two-beam test stand of the Compact Linear Collider test facility, Phys. Rev. ST Accel. Beams 14 (2011) 081001.

[11] T. Persson, Fighting Beam Instabilities At CTF3, Chalmers University of Technology, 2011.

[12] R.A. Fisher, Frequency distribution of the values of the correlation coefficient in samples from an indefinitely large population, Biometrika 10 (1915) 507–521.

[13] J. Mournier, R. Bossart, J.-M. Nonglaton, I. Syratchev, L. Tanner, Low level RF including a sophisticated phase control system for CTF3, in: LINAC'04, Lübeck, Germany, 2004, pp. 748–750.

[14] V.E. Balakin, I.V. Syrachev, Status of VLEPP RF power multiplier (VPM), in: EPAC'92, Berlin, Germany, 1992, pp. 1173–1175.

[15] A. Fiebig, R. Hohbach, Study of peak power doublers with spherical resonators, IEEE Trans. Nucl. Sci. 30 (1983) 3563–3565.

[16] A. Dubrovskiy, F. Tecker, RF pulse compression stabilization at the CTF3 CLIC Test Facility, in: IPAC'10, Kyoto, Japan, 2010, pp. 3774–3776.

[17] S.H. Shaker, R. Corsini, P.K. Skowronski, I. Syratchev, F. Tecker, Phase modulator programming to get flat pulses with desired length and power from the CTF3 pulse compressors, in: IPAC'10, Kyoto, Japan, 2010, pp. 1425–1427.

[18] T. Persson, P. Skowronski, R. Corsini, Drive beam stability studies and stabilization algorithms in CLIC test facility 3, Nucl. Instrum. Methods Phys. Res. A 735 (2014) 152–156.

[19] J. Roberts, P. Skowronski, P.N. Burrows, G.B. Christian, R. Corsini, A. Ghigo, F. Marcellini, C. Perry, Stabilization of the arrival time of a relativistic electron beam to the 50 fs level, Phys. Rev. Accel. Beams 21 (2018) 011001.

[20] E. Ikarios, A. Andersson, J. Barranco, B. Constance, R. Corsini, A. Gerbershagen, T. Persson, P.K. Skowronski, F. Tecker, The drive beam phase stability in CTF3 and its relation to the bunch compression factor, in: IPAC'13, Shanghai, China, 2013, pp. 1655–1657.